Official Journal of CIOMP
elight.springeropen.com

RESEARCH ARTICLE

Open Access

Real time full-color imaging in a Meta-optical fiber endoscope

Johannes E. Fröch[1,2*], Luocheng Huang[2], Quentin A.A. Tanguy[2], Shane Colburn[3], Alan Zhan[3], Andrea Ravagli[4], Eric J. Seibel[5], Karl F. Böhringer[2,6,7] and Arka Majumdar[1,2*]

Abstract

Endoscopes are an important component for the development of minimally invasive surgeries. Their size is one of the most critical aspects, because smaller and less rigid endoscopes enable higher agility, facilitate larger accessibility, and induce less stress on the surrounding tissue. In all existing endoscopes, the size of the optics poses a major limitation in miniaturization of the imaging system. Not only is making small optics difficult, but their performance also degrades with downscaling. Meta-optics have recently emerged as a promising candidate to drastically miniaturize optics while achieving similar functionalities with significantly reduced size. Herein, we report an inverse-designed meta-optic, which combined with a coherent fiber bundle enables a 33% reduction in the rigid tip length over traditional gradient-index (GRIN) lenses. We use the meta-optic fiber endoscope (MOFIE) to demonstrate real-time video capture in full visible color, the spatial resolution of which is primarily limited by the fiber itself. Our work shows the potential of meta-optics for integration and miniaturization of biomedical devices towards minimally invasive surgery.

Keywords Endoscopy, Meta-optics, Nano-fabrication, Biomedical engineering

1 Introduction

Ultra-compact, agile endoscopes with large field of view (FoV), long depth of field (DoF), and short rigid tip length are important tools for the development of minimally invasive operations and new experimental surgeries [1–6]. As these fields develop, the requirement on miniaturization and increased precision become progressively demanding. In existing endoscopes, a fundamental limitation of the device agility within small tortuous ducts, such as an artery, is the rigid tip length, which in turn is primarily constrained by the size of the optical elements required for imaging. Thus, alternative solutions are urgently needed to reduce the tip length [1].

Some of these solutions include lensless and computational imaging with single fibers [7–9] or coherent fiber bundles [10–13]. However, these are typically limited to a short working distance and often extremely sensitive to bending and twisting of the optical fiber, affecting, or even precluding accurate computational reconstruction. Moreover, the need for complex computational reconstruction often precludes real-time image capture. Additionally, different alternatives for optimizing [14], and fabricating compact optical elements have been studied, including 3D optical elements that can be directly printed on fibers [15], or freeform mirror optics for side-viewing endoscopes [16]. While high optical performance is reported, the scalability of 3D printed or freeform optical

*Correspondence:
Johannes E. Fröch
jfroech@uw.edu
Arka Majumdar
arka@uw.edu
[1] Department of Physics, University of Washington, Seattle, WA 98195, USA
[2] Department of Electrical and Computer Engineering, University of Washington, Seattle, WA 98195, USA
[3] Tunoptix, Fluke Hall, 4000 Mason Road 300, WA 98195 Seattle, USA
[4] SCHOTT North America, Inc., Southbridge, MA 01550, USA
[5] Department of Mechanical Engineering, University of Washington, Seattle, WA 98195, USA
[6] Department of Bioengineering, University of Washington, Seattle, WA 98195, USA
[7] Institute for Nano-Engineered Systems, University of Washington, Seattle, WA 98195, USA

elements remain elusive, which is an important consideration for endoscopy, where often disposable optics are preferred to avoid cross-contamination between patients.

An emerging and versatile idea in the photonics community to create miniaturized optical elements is flat meta-optics [17, 18]. These are sub-wavelength diffractive optical elements, composed of nano-scale scatterer arrays, designed to shape the phase, amplitude, and spectral response of an incident wavefront. Such ultrathin flat optics not only dramatically shrink the size of traditional optics, but can also combine multiple functionalities in a single surface [19–24]. Moreover, flat meta-optics are compatible with high-volume semiconductor manufacturing technology [25–27], and thus can create disposable optics. These properties have already inspired researchers to explore the potential of meta-optics for endoscopy including fiber-integrated endoscopy [28, 29], side-viewing single fiber scanning endoscopy [30], and scanning fiber forward viewing endoscopy [31]. Unfortunately, meta-optics traditionally suffer from strong aberrations (both chromatic and Seidel) making large FoV and full-color imaging challenging. Several works have shown that the common metalens design, a hyperboloid phase mask, is not suitable for simultaneously capturing color information across the visible spectrum, typically resulting in images, that are crisp for the design wavelength (e.g. green) but strongly aberrated/blurred for other colors (red, and blue) [32–34]. While dispersion engineering [35–38], and computational imaging techniques [19, 32, 34] can reduce chromatic aberration, they either suffer from small apertures, low numerical aperture [39, 40], or require a computational post-processing step, complicating real-time video capture. Similarly, an additional aperture in front of the meta-optic can provide a larger FoV [41, 42], but comes at the cost of reduced light collection and increased thickness of the optics. These limitations have so far restricted most meta-optics endoscopes primarily to single wavelength operation. One recent report, demonstrated a meta-optic doublet in conjunction with a coherent fiber bundle for polychromatic imaging (distinct wavelengths in the red, green, and blue band) [43]. However, such polychromatic imaging is not suitable for imaging under broadband illumination, which is often the case for clinical endoscopy. Additionally, the front aperture was limited to 125 μm, with a short working distance of 200 μm. We note that, while we do want small aperture meta-optics for endoscopy, making it smaller than the optical fiber diameter is not conducive and severely limits the light collection. Researchers also recently demonstrated achromatic imaging in a meta-optics integrated fiber, but this was done in the infrared regime with a fractional bandwidth of ~ 0.27 $(1.25 - 1.65\mu m)$ [28]. As such full-color meta-optical endoscopy (between 400 and 700 nm, a fractional bandwidth of ~ 0.54) with acceptable FoV, DoF and large enough aperture has not yet been achieved.

In this work, we demonstrate an inverse-designed meta-optic, optimized to capture real-time full-color scenes in the visible in conjunction with a 1 mm diameter coherent fiber bundle (Fig. 1). The meta-optic enables operations at a FoV of 22.5^o, a DoF of >30 mm (exceeding 300% of the nominal design working distance) and a

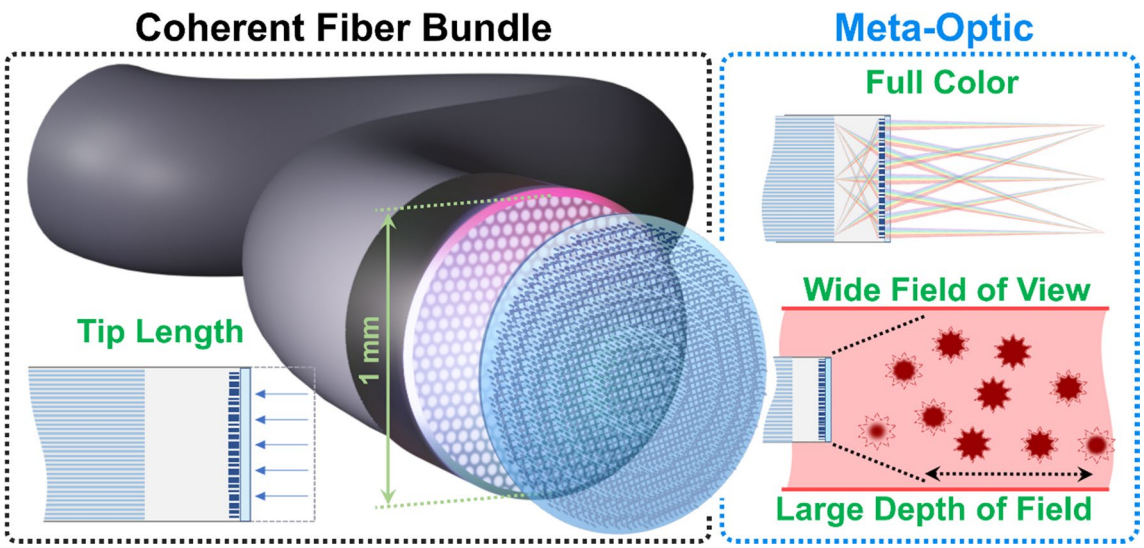

Fig. 1 Schematic of the meta-optical fiber endoscope: the meta-optics is optimized to have a large average volume under the MTF curve over a broad wavelength range to allow color preservation. In comparison with a traditional GRIN lens, the use of meta-optics reduces the tip length, while maintaining a wide field of view of $22.5^o$and large depth of field exceeding 30 mm

minimum rigid tip length of only ~ 2.5 mm (effective NA of 0.24). Compared to a traditional commercial gradient-index (GRIN) lens integrated fiber bundle endoscope, this is a 33% tip length reduction, thanks to the shorter focal length and the ultrathin nature of the meta-optic, while at the same time comparable imaging performance and working distance are maintained. To achieve exceptional FoV, DoF, and color performance of the Meta-Optical Fiber Endoscope (MOFIE), we approached this design problem from a system level perspective, considering that the diameter and spacing of individual fiber cores within the bundle limit the achievable image quality, which in turn also limits the achievable FoV and modulation transfer function (MTF) [6]. This aspect is implemented in an automatic differentiation framework using the average volume under the multichromatic, modulation transfer function (MTF) curve as the figure of merit. The design algorithm is further detailed in the Additional file 1. By ensuring that the meta-optic has a MTF within the limit posed by the fiber bundle, we achieve full color operation without the requirement of a computational reconstruction step, thus facilitating real time operation. We emphasize that our design approach is fundamentally different from traditional achromatic metalens design effort. Instead of trying to achieve diffraction limited performance in all wavelengths, which may pose a physically unsolvable problem [39], we formulate an optimization problem that can find the best possible solution for full-color imaging. An important aspect of this approach is that it is not limited to this particular system, but can be extended to larger aperture sizes and also support computational post processing steps. To highlight this, we have added an example of a meta-optic with 1 cm aperture, demonstrating full color imaging under ambient light conditions.

2 Results

A defining limitation of meta-optics is their chromatic aberration [44]. Whereas a hyperboloid meta-lens can have diffraction-limited performance at the design wavelength, the MTF degrades rapidly for operation over an extended spectral range [40]. To tackle this issue, we use an inverse design approach, which maximizes the volume under a multi-chromatic MTF curve as the figure of merit during the optimization. Our figure of merit also ensures that the MTF remains similar over a broad wavelength range, which is critical for broadband operation (detailed in the Additional file 1). To ensure polarization-insensitive operation and compatibility with high volume manufacturing processes, the specific design is implemented through simple square pillars with a minimum feature size of 75 nm and a maximum aspect ratio of 10 (detailed in the Additional file 1).

We fabricated the 1 mm aperture f/2 meta-optic in SiN, due to its high transparency in the visible wavelength range (details in Methods) and wide availability of thin films grown by plasma-enhanced chemical vapor deposition on quartz [25]. An optical image (Fig. 2a) shows that the device integrity is maintained throughout the entire area, exhibited by the same structural color for specific radii of the meta-optic stemming from a radial-symmetric design constraint. Further inspection with a scanning electron microscope of the meta-optic (Fig. 2b, c) shows the scatterer quality of a representative device area,

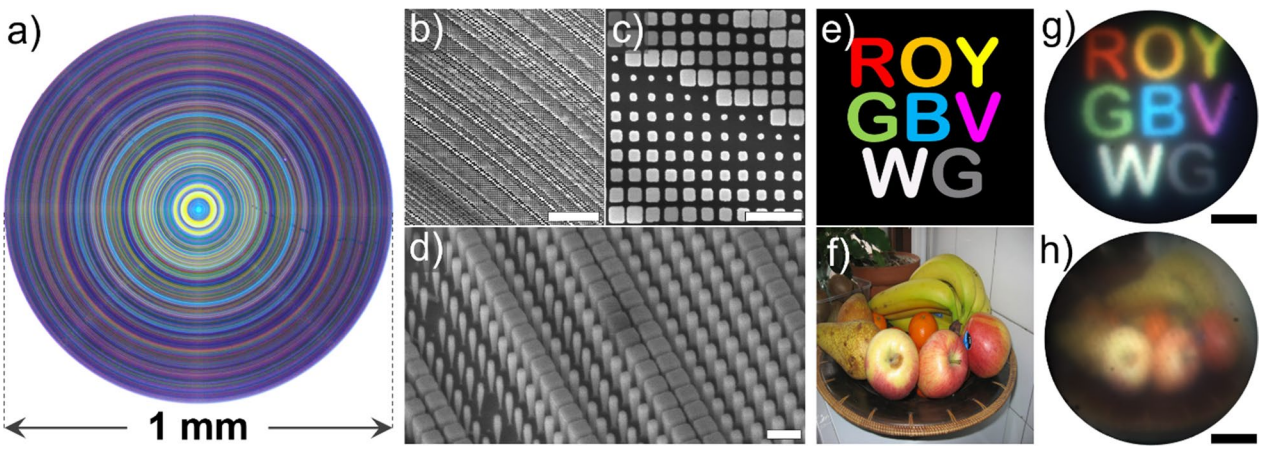

Fig. 2 Characterization of the meta-optic. **a** Optical microscope image of the 1 mm aperture meta-optic. Different colors of the device correspond to different regions of pillars, which exhibit a structural color effect. **b**, **c** Top view SEM images of the fabricated device. Scale bars correspond to 10 µm and 1 µm, respectively. **d** SEM image at an oblique angle of 45°. The scale bar corresponds to 500 nm. **e**, **f** Full color scenes displayed on an OLED screen. **g**, **h** Corresponding images captured with the MOFIE at working distance of 10 mm. Scale bars correspond to 1 mm. Images displayed are without any computational deconvolution

highlighting the successful fabrication of the individual elements with the desired footprint and aspect ratio, as well as negligible sidewall roughness (Fig. 2d). Detailed characterization, such as the point spread function (PSF) and the MTF of the stand- alone meta-optic can be found in the Additional file 1.

For a demonstration of the MOFIE, we placed an OLED screen in front of the meta-optic at the proximal end of the CFB and a capturing system at its distal end, consisting of an objective, tube lens, and camera. The setup is further detailed in the methods section and schematically depicted in the Additional file 1. A set of multicolored images were then displayed on the OLED screen (Fig. 2e, f) and captured through the MOFIE as shown in Fig. 2g, h. Importantly, the color quality is entirely preserved throughout the visible range, even for more complex scenes (Fig. 2f, h), while maintaining a reasonable resolution. This is relevant, because common metalens designs (such as a hyperboloid) are well known to have a very strong chromatic aberration, which precludes full-color operation over the entire visible wavelength range. Yet, medical surgery requires high quality color reproduction to confidently discern diseased tissue.

We emphasize here that in comparison to many prior works [19, 32, 33, 45], the presented images were not computationally deconvolved to enhance the image quality. However, an artificial blur was added to reduce visual moiré pattern artefacts due to the noticeable fiber core size, as discussed in the Additional file 1.

In the following we characterized the performance of the MOFIE, with respect to its FoV, DoF, and spatial resolution using the previously described imaging configuration. The results are summarized in Fig. 3.

First, from a measurement of a checkerboard pattern (Fig. 3a, b), at a working distance of 10 mm, we determined the FoV to be ~ 22.5°. In context, this still allows to view an object area with a field of view of ~ 4 mm at a working distance of 10 mm. This is relevant because the average diameter of several important human arteries (e.g. coronary, cerebral) are on the order of ~ 1–3 mm [46, 47]. Hence the MO endoscope completely covers the entire relevant cross section that will be under investigation during operation.

A further important factor for endoscope imaging is the DoF, because *in-vivo* movements such as a beating heart or breathing lung, can significantly change the working distance within tens of milliseconds, making a large DoF extremely beneficial. To evaluate the performance in this regard, we placed the OLED screen at different working distances of the respective endoscope, while displaying the same images, at working distances of 7 mm, 10 mm (design working distance), 18 mm, and 40 mm (intermediates are shown in the Additional file 1). This was done while maintaining the same distance between the coherent fiber bundle and meta-optic. Importantly, it can be clearly seen from the image series (Fig. 3c–e) that throughout this range of 33 mm the same sharpness and color quality is achieved.

To quantitatively assess the imaging resolution at the design working distance (10 mm), we placed a USAF Target in front of the MOFIE, which was illuminated by a broadband halogen source from a second fiber

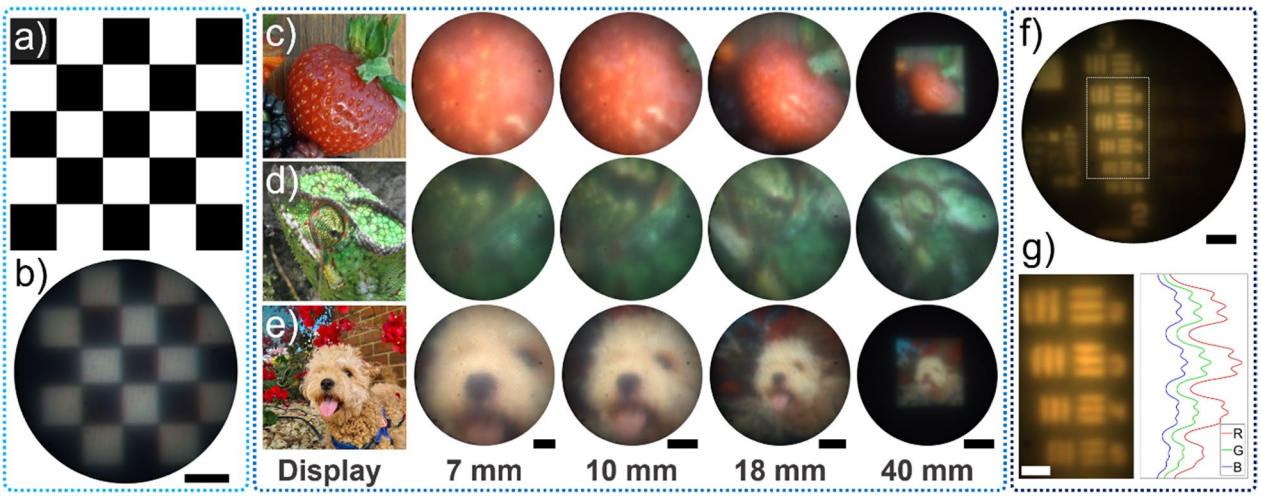

Fig. 3 Assessment of the MOFIE. **a** A checkerboard pattern as displayed on a screen with a width of 4 mm. **b** Captured image through the MOFIE at a working distance of 10 mm. Scale bar correspond to 1 mm. **c**, **d** and **e**, show images that were displayed on an OLED screen and captured at working distances of 7 mm (scale bar of 0.5 mm), 10 mm (scale bar of 0.5 mm), 18 mm (scale bar of 1 mm), and 40 mm (scale bar of 2.5 mm). **f** Captured image of the group 3 lines of a USAF 1951 resolution chart. Scale bar corresponds to 0.5 mm (**g**) shows a magnified image of elements 2–5, with a line profile of the red (R), green (G), and blue (B) channels. Scale bar corresponds to 250 µm

placed next to the CFB. A captured image of the group 3 elements is shown in Fig. 3f. A magnified image in 3 g, shows the attainable resolution down to elements 3 and 4, indicating a line resolution of ~ 50 µm. An important aspect is that the individually resolved color channels show the same resolution throughout, indicated by similar lines profiles. We note that the yellowish tint in the captured images stems from the spectral distribution of the broad band halogen source (see Additional file 1), which however can be rebalanced on the image display or resolved using a spectrally equal distributed light source.

To emphasize the capabilities of the MOFIE we demonstrate real-time, full-color imaging of a biological sample, shown in Fig. 4. This is an important step, because in-the-field deployment of an endoscope ultimately requires imaging capabilities with video-rate speed while maintaining full-color information. We emphasize that complicated computational imaging approaches, such as the ones used with lensless imaging may preclude video-rate imaging. To emulate such a situation under the given requirements, we recorded the movement of a living caterpillar on top of a strawberry leaf at a video rate of ~ 14 frames-per-second at a working distance of ~ 10 mm (a picture of the image scene is shown in the Additional file 1). For illumination of the scene, we used a broadband tungsten-halogen source, which was coupled into an optical fiber, placed next to the coherent fiber bundle pointing towards the scene.

In Fig. 4, a frame series is shown as the caterpillar moves across the leaf, the full movie can be found in the Additional file 1. We note that no deconvolution of the images was applied, and the shown frames are equivalent to the imaging that was displayed on the image capture tool during this experiment. We emphasize here that this recording is in fact to our knowledge, one of the first demonstrations of full-color video-rate imaging using a meta-optic, which further highlights a relevant advancement in this field. Although some other works have demonstrated frame series acquired using a meta-optic, these were small apertures meta-optics.

(~ 100 µm) with much lower NA (0.1) and required further relay optics for acquisition and a computational post rendering step [36, 48] or were designed for distinct wavelengths [49, 50].

3 Discussion

To assess the performance metrics of the MOFIE relative to an established system, we further compared it with a commercial state-of-the-art graded index (GRIN) lens-based endoscope. A comparison of images that were displayed on the OLED screen and images that were captured either with the MOFIE or the GRIN endoscope are summarized in the Additional file 1.

We reduced the optical tip length from 3.75 mm for a GRIN lens-based endoscope by 33% down to 2.5 mm, for the MOFIE. We note that the tip length in MOFIE can be readily reduced further by using a thinner carrier substrate (100 µm instead of 500 µm). Although, the image quality of the MOFIE appears with some residual haze in comparison to the GRIN lens-based endoscope, due to a larger tail in the broadband PSF (see Additional file 1), it still is capable of broadband and full color imaging, with a resolution of ~ 50 µm, and up to 4 mm object size, at 10 mm working distance. The FoV of the MOFIE is 22.5° compared to 45° for the GRIN lens-based endoscope. In contrast, we achieve a better DoF perception over the characterized working distance range (~ 30 mm) over the GRIN lens (DoF ~ 13 mm). While we used a benchtop configuration in the current demonstration, future effort will focus on full integration with a coherent fiber bundle and direct medical demonstrations to illustrate the full power of the MOFIE. This will require significant effort on integration and will thus be a topic of future work, which will also enable to evaluate the mechanical

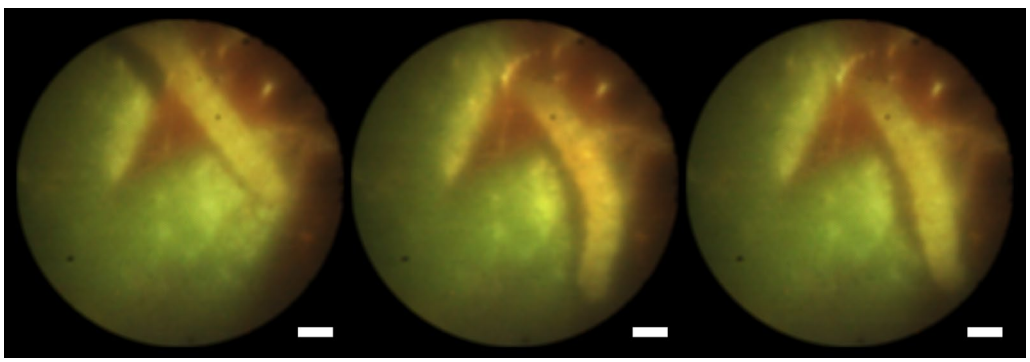

Fig. 4 Clip of a full color video rate imaging of a caterpillar on a strawberry leaf. Observation of a crawling movement of the caterpillar across a gap in the strawberry leaf. White scale bars correspond to 500 µm. A yellowish tint on the captured video appeared due to the spectral distribution of the used light source (a spectrum of the light source is shown in Additional file 1)

performance of the MOFIE, such as the bendability. Beyond that, multiple pathways could be pursued integrating meta-optics with coherent fiber bundles. Specifically, a suitable computational backend might further improve the image quality or an arrayed meta-optics [51] could enable an ultra large FoV or foveated imaging. Especially the latter would facilitate a reduction in the optical track length and would thus be an attractive option to further reduce the rigid tip length. Instead of a single lens with an aperture of 1 mm and focusing distance of ~2 mm to the fiber bundle, the system would consist of multiple apertures, each optimized for a specific section of the field of view and shorter focusing distance into the fiber bundle, thus minimizing the optical track length/rigid tip length. Although a smaller aperture would trade off lower collected signal intensity, it could be compensated with an improved illumination.

Among existing types of fiber-based endoscopes, we chose to optimize a meta-optic for direct full color imaging in combination with a CFB. In contrast, single fiber-based systems, such as scanning fiber endoscopes [31] can provide a thinner diameter of the device but require a sophisticated scanning mechanism at the tip of the endoscope. CFB-based endoscopes on the other hand require a typically thicker diameter, but no scanning element is required.

Because the ultimate limit on imaging resolution is dictated by the number of fibers within the bundle, a strict trade-off exists between working distance, DoF, resolution, and FoV, further restricted by the acceptance NA of the fibers within the bundle. Therefore, a larger FoV typically results in a lower resolution. However, the exact needs may vary depending on the type of endoscopy and whether extended analytical capabilities are required. For instance, a large FoV might be more favorable over a higher resolution when simultaneous coordination with other tools is required. At the same time a specific working distance with a large DoF might be more appealing for applications where the working distance changes rapidly, such as moving parts (e.g., a beating heart) in the body. However, in all cases a tip length will be beneficial, which is demonstrated in our paper. Especially, with evolution of this field, new research problems, such as optimizing application-specific meta-optics for a given endoscopic applications, are expected to emerge.

4 Conclusion

In summary, we have demonstrated real-time, full-color operation of a meta-optic fiber endoscope (MOFIE). Approaching this problem from a system level design perspective, we created a meta-optic that is specifically suited for operation in combination with the optical constraints of a coherent fiber bundle. Specifically, as the spatial resolution of MOFIE is limited by the coherent fiber bundle, the meta-optic is optimized to have an MTF sufficient to image through the fiber bundle. Thus, the combined system facilitates full-color, video-rate imaging, which could be potentially further improved using a computational backend. However, in this case a considerable optimized algorithm computer hardware would be required to avoid any lag during operation of the MOFIE.

The fabricated meta-optic has a device length of 2.5 mm, which is a reduction of ~33% to a comparable GRIN lens (3.75 mm). We demonstrate a 22.5° field of view, >30 mm depth of field, and real time, full color imaging, highlighted by video recordings of a biological sample. To the best of our knowledge the present work presents one of the first applications, where a meta-optic is used for full color and real time imaging simultaneously. Beyond that, our work exemplifies where meta-optics can potentially find a strong position in biomedical applications with drastically reduced imaging system size.

5 Methods

5.1 Fabrication

For fabrication, we first deposited a ~750 nm thick SiN film on a 500 µm thick quartz wafer using plasma enhanced chemical vapor deposition (PECVD) in a SPTS PECVD chamber. A positive resist (ZEP 520 A) was then spun onto the wafer, followed by baking at 180 °C for 3 min. To minimize charging effects during patterning, a conductive polymer layer (DisCharge H2O) was subsequently spun on top. The resist layer was then patterned using a 100 kV electron beam (JEOL JBX6300FS) at a dose of ~300 µC cm^{-2} and developed in Amyl Acetate for 2 min. Then a layer (~50 nm) of AlO_x was deposited using electron beam evaporation. After overnight lift-off in NMP, the SiN layer was etched using a mixture of C_4F_8/SF_6 in an inductively coupled reactive ion etcher (Oxford PlasmaLab System 100). For SEM imaging a thin conductive Au/Pd layer was deposited.

5.2 Measurements

The measurement setup consisted of an OLED screen, the meta-optic element and the CFB (SCHOTT RLIB CVET, 1.05×910, 7.6 M, 18K19, QA.90). The imaging setup at the distal end of the CFB consisted of an objective lens (Nikon), a tube lens (Thorlabs), and a camera (Allied Vision GT 1930 C). In configurations where the USAF 1951 target was imaged, or for video recording, the sample was illuminated with a broadband halogen source (Thorlabs SLS301), which was delivered and directed towards the sample through a multimode fiber (core size 200 µm). The fiber was placed next to the CFB, which would be a typical configuration for an endoscope. For comparison with a GRIN lens endoscope, a GRIN lens

(GoFoton) with 1.3 mm lens diameter, length of 3.75 mm, and working distance of 10 mm was attached to the CFB.

During processing of the acquired images, we have only adjusted the brightness, as well as adding a slight blur to the image to minimize artificial moiré patterns that would otherwise emerge due to the periodic arrangement of the fiber cores in the CFB. Such a slight deblur, however, could also be achieved by adjusting the output facet of the fiber relative to the imaging system. A comparison is shown in the Additional file 1.

Supplementary Information

The online version contains supplementary material available at https://doi.org/10.1186/s43593-023-00044-4.

Additional file 1: Real Time Full-Color Imaging in a Meta-Optical Fiber Endoscope.

Author contributions

AM conceived the idea. LH designed the meta-optics. QT and JF fabricated the meta-optics. SC, AZ, JF measured the meta-optics with coherent fiber bundle. AR and ES provided expertise on endoscopy. AM and KB supervised the project. JF and AM wrote the manuscript with input from everyone. All authors read and approved the final manuscript.

Funding

This research was supported by NSF-GCR-2120774. Part of this work was conducted at the Washington Nanofabrication Facility/Molecular Analysis Facility, a National Nanotechnology Coordinated Infrastructure (NNCI) site at the University of Washington with partial support from the National Science Foundation via awards NNCI-1542101 and NNCI-2025489.

Availability of data and materials

The data that support the findings of this study are available from the corresponding author upon reasonable request.

Declarations

Competing interests

A.M., K.B, S.C., A.Z. are involved in Tunoptix, who is trying to commercialize related technology.

Received: 6 December 2022 Revised: 11 April 2023 Accepted: 15 April 2023
Published online: 07 June 2023

References

1. B.A. Flusberg, E.D. Cocker, W. Piyawattanametha, J.C. Jung, E.L.M. Cheung, M.J. Schnitzer, Fiber-optic fluorescence imaging. Nat. Methods **2**, 941–950 (2005)
2. C.M. Lee, C.J. Engelbrecht, T.D. Soper, F. Helmchen, E.J. Seibel, Scanning fiber endoscopy with highly flexible, 1 mm catheterscopes for wide-field, full-color imaging. J. Biophotonics **3**, 385–407 (2010)
3. A. Perperidis, K. Dhaliwal, S. McLaughlin, T. Vercauteren, Image computing for fibre-bundle endomicroscopy: a review. Med. Image. Anal **62**, 101620 (2020)
4. A. Shadfan, A. Hellebust, R. Richards-Kortum, T. Tkaczyk, Confocal foveated endomicroscope for the detection of esophageal carcinoma. Biomed. Opt. Express BOE **6**, 2311–2324 (2015)
5. A. Shadfan, H. Darwiche, J. Blanco, A. Gillenwater, R. Richards-Kortum, T.S. Tkaczyk, Development of a multimodal foveated endomicroscope for the detection of oral cancer. Biomed. Opt. Express BOE **8**, 1525–1535 (2017)
6. J. Park, D.J. Brady, G. Zheng, L. Tian, L. Gao, Review of bio-optical imaging systems with a high space-bandwidth product. A.P **3**, 044001 (2021)
7. P. Caramazza, O. Moran, R. Murray-Smith, D. Faccio, Transmission of natural scene images through a multimode fibre. Nat. Commun. **10**, 2029 (2019)
8. Z. Liu, L. Wang, Y. Meng, T. He, S. He, Y. Yang, L. Wang, J. Tian, D. Li, P. Yan, M. Gong, Q. Liu, Q. Xiao, All-fiber high-speed image detection enabled by deep learning. Nat. Commun. **13**, 1433 (2022)
9. L. Wang, Y. Yang, Z. Liu, J. Tian, Y. Meng, T. Qi, T. He, D. Li, P. Yan, M. Gong, Q. Liu, Q. Xiao, High-speed all-Fiber micro-imaging with large depth of field. Laser Photonics Rev **16**, 2100724 (2022)
10. J. Shin, D.N. Tran, J.R. Stroud, S. Chin, T.D. Tran, M.A. Foster, A minimally invasive lens-free computational microendoscope. Sci. Adv **5**, eaaw5595 (2019)
11. N. Badt, O. Katz, Real-time holographic lensless micro-endoscopy through flexible fibers via fiber bundle distal holography. Nat. Commun. **13**, 6055 (2022)
12. A. Orth, M. Ploschner, E.R. Wilson, I.S. Maksymov, B. C. Gibson, Optical fiber bundles: ultra-slim light field imaging probes. Sci. Adv **5**, eaav1555 (2019)
13. W. Choi, M. Kang, J.H. Hong, O. Katz, B. Lee, G.H. Kim, Y. Choi, W. Choi, Flexible-type ultrathin holographic endoscope for microscopic imaging of unstained biological tissues. Nat. Commun. **13**, 4469 (2022)
14. H. Li, Z. Hao, J. Huang, T. Lu, Q. Liu, L. Fu, 500 μm field-of-view probe-based confocal microendoscope for large-area visualization in the gastrointestinal tract. Photon Res. PRJ **9**, 1829–1841 (2021)
15. T. Gissibl, S. Thiele, A. Herkommer, H. Giessen, Two-photon direct laser writing of ultracompact multi-lens objectives. Nat. Photon **10**, 554–560 (2016)
16. J. Li, S. Thiele, B.C. Quirk, R.W. Kirk, J.W. Verjans, E. Akers, C.A. Bursill, S.J. Nicholls, A.M. Herkommer, H. Giessen, R.A. McLaughlin, Ultrathin monolithic 3D printed optical coherence tomography endoscopy for preclinical and clinical use. Light Sci. Appl. **9**, 124 (2020)
17. N. Yu, F. Capasso, Flat optics with designer metasurfaces. Nat. Mater **13**, 139–150 (2014)
18. M.K. Chen, Y. Wu, L. Feng, Q. Fan, M. Lu, T. Xu, D.P. Tsai, Principles, functions, and applications of Optical Meta-Lens. Adv. Opt. Mater. **9**, 2001414 (2021)
19. S. Colburn, A. Zhan, A. Majumdar, Metasurface optics for full-color computational imaging. Sci. Adv **4**, eaar2114 (2018)
20. C. Munley, W. Ma, J.E. Fröch, Q.A.A. Tanguy, E. Bayati, K.F. Böhringer, Z. Lin, R. Pestourie, S.G. Johnson, A. Majumdar, Inverse-designed meta-optics with spectral-spatial engineered response to mimic color perception. Adv. Opt. Mater **10**, 2200734 (2022)
21. A. Arbabi, Y. Horie, M. Bagheri, A. Faraon, Dielectric metasurfaces for complete control of phase and polarization with subwavelength spatial resolution and high transmission. Nat. Nanotech **10**, 937–943 (2015)
22. M. Piccardo, V. Ginis, A. Forbes, S. Mahler, A.A. Friesem, N. Davidson, H. Ren, A.H. Dorrah, F. Capasso, F.T. Dullo, B.S. Ahluwalia, A. Ambrosio, S. Gigan, N. Treps, M. Hiekkamäki, R. Fickler, M. Kues, D. Moss, R. Morandotti, J. Riemensberger, T.J. Kippenberg, J. Faist, G. Scalari, N. Picqué, T.W. Hänsch, G. Cerullo, C. Manzoni, L.A. Lugiato, M. Brambilla, L. Columbo, A. Gatti, F. Prati, A. Shiri, A.F. Abouraddy, A. Alù, E. Galiffi, J.B. Pendry, P.A. Huidobro, Roadmap on multimode light shaping. J. Opt. **24**, 013001 (2021)
23. S.C. Malek, A.C. Overvig, A. Alù, N. Yu, Multifunctional resonant wavefront-shaping meta-optics based on multilayer and multi-perturbation nonlocal metasurfaces. Light Sci. Appl. **11**, 246 (2022)
24. Z. Lin, R. Pestourie, C. Roques-Carmes, Z. Li, F. Capasso, M. Soljačić, M. Soljačić, S.G. Johnson, End-to-end metasurface inverse design for single-shot multi-channel imaging. Opt. Express OE **30**, 28358–28370 (2022)
25. S. Colburn, A. Zhan, E. Bayati, J. Whitehead, A. Ryou, L. Huang, A. Majumdar, Broadband transparent and CMOS-compatible flat optics with silicon nitride metasurfaces [Invited]. Opt. Mater. Express OME **8**, 2330–2344 (2018)
26. J.-S. Park, S. Zhang, A. She, W.T. Chen, P. Lin, K.M.A. Yousef, J.-X. Cheng, F. Capasso, All-Glass, large metalens at visible Wavelength using Deep-Ultraviolet Projection Lithography. Nano Lett. **19**, 8673–8682 (2019)

27. L. Zhang, S. Chang, X. Chen, Y. Ding, M.T. Rahman, Y. Duan, M. Stephen, X. Ni, High-Efficiency, 80 mm aperture Metalens Telescope. Nano Lett. **23**, 51–57 (2023)
28. H. Ren, J. Jang, C. Li, A. Aigner, M. Plidschun, J. Kim, J. Rho, M.A. Schmidt, S.A. Maier, An achromatic metafiber for focusing and imaging across the entire telecommunication range. Nat. Commun. **13**, 4183 (2022)
29. M. Plidschun, H. Ren, J. Kim, R. Förster, S.A. Maier, M.A. Schmidt, Ultrahigh numerical aperture meta-fibre for flexible optical trapping. Light Sci. Appl. **10**, 57 (2021)
30. H. Pahlevaninezhad, M. Khorasaninejad, Y.-W. Huang, Z. Shi, L.P. Hariri, D.C. Adams, V. Ding, A. Zhu, C.-W. Qiu, F. Capasso, M.J. Suter, Nano-optic endoscope for high-resolution optical coherence tomography in vivo. Nat. Photon **12**, 540–547 (2018)
31. N. Xie, M.D. Carson, J.E. Fröch, A. Majumdar, E. Seibel, K.F. Böhringer, Large FOV short-wave infrared meta-lens for scanning fiber endoscopy. arXiv (2022). https://doi.org/10.48550/arXiv.2212.11272
32. E. Tseng, S. Colburn, J. Whitehead, L. Huang, S.-H. Baek, A. Majumdar, F. Heide, Neural nano-optics for high-quality thin lens imaging. Nat. Commun. **12**, 6493 (2021)
33. L. Huang, J. Whitehead, S. Colburn, A. Majumdar, A. Majumdar, Design and analysis of extended depth of focus metalenses for achromatic computational imaging. Photon Res. PRJ **8**, 1613–1623 (2020)
34. L. Huang, S. Colburn, A. Zhan, A. Majumdar, Full-Color metaoptical imaging in visible light. Adv. Photo. Res. (2022). https://doi.org/10.1002/adpr.202100265
35. W.T. Chen, A.Y. Zhu, V. Sanjeev, M. Khorasaninejad, Z. Shi, E. Lee, F. Capasso, A broadband achromatic metalens for focusing and imaging in the visible. Nat. Nanotech **13**, 220–226 (2018)
36. S. Wang, P.C. Wu, V.-C. Su, Y.-C. Lai, M.-K. Chen, H.Y. Kuo, B.H. Chen, Y.H. Chen, T.-T. Huang, J.-H. Wang, R.-M. Lin, C.-H. Kuan, T. Li, Z. Wang, S. Zhu, D.P. Tsai, A broadband achromatic metalens in the visible. Nat. Nanotech **13**, 227–232 (2018)
37. W.T. Chen, A.Y. Zhu, F. Capasso, Flat optics with dispersion-engineered metasurfaces. Nat. Rev. Mater. **5**, 604–620 (2020)
38. W. Zang, Q. Yuan, R. Chen, L. Li, T. Li, X. Zou, G. Zheng, Z. Chen, S. Wang, Z. Wang, S. Zhu, Chromatic dispersion manipulation based on Metalenses. Adv. Mater **32**, 1904935 (2020)
39. F. Presutti, F. Monticone, Focusing on bandwidth: achromatic metalens limits. Optica **7**, 624–631 (2020)
40. J. Engelberg, U. Levy, Achromatic flat lens performance limits. Optica **8**, 834–845 (2021)
41. M.Y. Shalaginov, S. An, F. Yang, P. Su, D. Lyzwa, A.M. Agarwal, H. Zhang, J. Hu, T. Gu, Single-element diffraction-limited fisheye metalens. Nano Lett **20**, 7429–7437 (2020)
42. J. Engelberg, C. Zhou, N. Mazurski, J. Bar-David, A. Kristensen, U. Levy, Near-IR wide-field-of-view Huygens metalens for outdoor imaging applications. Nanophotonics **9**, 361–370 (2020)
43. Y. Liu, Q.-Y. Yu, Z.-M. Chen, H.-Y. Qiu, R. Chen, S.-J. Jiang, X.-T. He, X.-T. He, F.-L. Zhao, F.-L. Zhao, J.-W. Dong, Meta-objective with sub-micrometer resolution for microendoscopes. Photon Res. PRJ **9**, 106–115 (2021)
44. E. Arbabi, A. Arbabi, S.M. Kamali, Y. Horie, A. Faraon, Multiwavelength polarization-insensitive lenses based on dielectric metasurfaces with meta-molecules. Optica **3**, 628–633 (2016)
45. E. Bayati, R. Pestourie, S. Colburn, Z. Lin, S.G. Johnson, A. Majumdar, Inverse designed extended depth of focus meta-optics for broadband imaging in the visible. Nanophotonics (2021). doi:https://doi.org/10.1515/nanoph-2021-0431
46. P. Mouches, N.D. Forkert, A statistical atlas of cerebral arteries generated using multi-center MRA datasets from healthy subjects. Sci. Data **6**, 29 (2019)
47. J.T. Dodge Jr, B.G. Brown, E.L. Bolson, H.T. Dodge, Lumen diameter of normal human coronary arteries. Influence of age, sex, anatomic variation, and left ventricular hypertrophy or dilation. Circulation **86**, 232–246 (1992)
48. R.J. Lin, V.-C. Su, S. Wang, M.K. Chen, T.L. Chung, Y.H. Chen, H.Y. Kuo, J.-W. Chen, J. Chen, Y.-T. Huang, J.-H. Wang, C.H. Chu, P.C. Wu, T. Li, Z. Wang, S. Zhu, D.P. Tsai, Achromatic metalens array for full-colour light-field imaging. Nat. Nanotechnol **14**, 227–231 (2019)
49. Z. Li, R. Pestourie, J.-S. Park, Y.-W. Huang, S.G. Johnson, F. Capasso, Inverse design enables large-scale high-performance meta-optics reshaping virtual reality. Nat. Commun. **13**, 2409 (2022)
50. W. Feng, J. Zhang, Q. Wu, A. Martins, Q. Sun, Z. Liu, Y. Long, E.R. Martins, J. Li, H. Liang, RGB achromatic metalens doublet for digital imaging. Nano Lett **22**, 3969–3975 (2022)
51. J. Chen, J. Chen, X. Ye, X. Ye, S. Gao, S. Gao, Y. Chen, Y. Chen, Y. Zhao, Y. Zhao, C. Huang, K. Qiu, S. Zhu, S. Zhu, T. Li, T. Li, Planar wide-angle-imaging camera enabled by metalens array. Optica **9**, 431–437 (2022)